Proceedings of The Institute of Acoustics

NONLINEAR EFFECTS WITH FOCUSSED ULTRASOUND IN TISSUES:AN IMPROVED MODEL

W. Swindell

Joint Department of Physics, Institute of Cancer Research and Royal Marsden Hospital, Downs Road, Sutton, Surrey, SM2 5PT, UK.

INTRODUCTION

An initially harmonic, longitudinal acoustic wave necessarily distorts as it propagates because of the accompanying density fluctuations in the medium. In tissue-like media, the beam energy is attenuated (absorbed) more rapidly than it otherwise would be for two reasons. First the distortion process removes energy from the fundamental (first harmonic) and transfers it to higher harmonics. There is no loss associated with the conversion process, but if the absorption coefficient of the fluid or tissue exhibits the usual power law variation with frequency, then the beam energy will be absorbed more rapidly because of the higher frequency components. Second, if conditions permit a shock wave to develop, there are additional losses associated with the irreversible nature of the shock. These losses take place even in so-called 'lossless fluids' and are described by the Rankine-Hugoniot equations. Clinical hyperthermia for treatment of malignant disease is an obvious application where it may be possible to exploit this enhanced deposition of energy. In a previous paper [1] the author analysed the deposition of thermal energy associated with the nonlinear propagation of an intense, focused ultrasound beam through tissue-like absorbing media. According to the theoretical model employed it was predicted that under certain circumstances, the amount of heat that could be deposited exceeded that which would be expected if nonlinear effects were not present by a significant amount. Figure 1 shows a result from that paper. Curves (a) - (e) show this enhancement of the absorbed power density (expressed as a ratio) for five different beam diameters. The (Gaussian) diameter of the beam at the transducer varies from 0.08 metres (a) to 0.16 metres (e) in steps of 0.02 metres. In this example the transducer had a radius of curvature of 0.16 metres, the axial intensity of ultrasound of the transducer was 10^5 watt per metre^2, the fundamental frequency was 1 MHz and there was a water path of 0.06 metres.

Figure 1

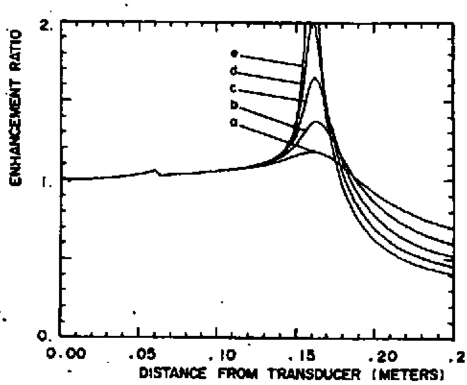

METHODS

In [1] it was assumed that the transducer emitted a Gaussian wavefront. This avoids the complexities of the diffraction pattern of the uniform circular wavefront. In the paraxial limit the Gaussian wave is described by its complex velocity amplitude $u_g(r)$ in the plane $z = z_1$ by

$$u_g(r) = u(0)\exp[-\pi(r^2/b_1^{\,2})]\ \exp(-i\pi r^2/\lambda R_1)$$
$$\times \exp(-ikz)\ \exp(i\phi_z) \qquad (1)$$

where r is the radial distance. The first exponential term describes the Gaussian radial dependence of the amplitude; b_1 is the radius at which the amplitude has fallen to 4.3% of its axial value and 81% of the beam power is contained within this radius. The second exponential term shows the wave to be a spherical wave whose radius of curvature is R_1. The beam is converging for $R_1 < 0$. The remaining terms will be discussed later. The essential property of a Gaussian wave is that it remains a Gaussian wave as it propagates. At z_2 the Gaussian parameters b_2 and R_2 are:

$$b_2 = b_1[1 + \epsilon_1)q_{1,2}^{\,2} + 2q_{1,2} + 1]^{1/2} \qquad (2)$$

$$R_2 = R_1\left[\frac{(1 + \epsilon_1)q_{1,2}^{\,2} + 2q_{1,2} + 1}{(1 + \epsilon_1)q_{1,2} + 1}\right] \qquad (3)$$

where

$$q_{1,2} = (z_2 - z_1)/R_1 \qquad (4)$$

and

$$\epsilon_1 = (\lambda R_1/b_1^{\,2})^2 \qquad (5)$$

The location of the beam waist and beam waist radius are given by:

$$z_w = z_1 - R_1/(1 + \epsilon_1) \qquad (6)$$

and

$$b_w = b_1[\epsilon_1(1 + \epsilon_1)]^{1/2} \qquad (7)$$

The phase angle ϕ_z in eqn (10) is given by

$$\tan\phi_z = (z - z_w)\lambda/b_w^{\,2} \qquad (8)$$

Thus the third and fourth terms of eqn (1) show linear phase propagation together with a nonlinear change of π which takes place symmetrically about and largely within a distance of $\pm b_w^2/\lambda$ from z_w. The advantage of using this type of wave is that the beam passes through the focal zone in a smooth manner, and the radius of curvature R does not vanish at the waist. Rather, it achieves some minimum value on either side of the waist.

The creation of harmonic amplitudes, u_n, is governed by the rate equation:

$$\frac{du_n(z)}{dz} = \frac{\omega\beta}{2c_o^2}\left[\sum_{j=1}^{n-1} j u_j(z) u_{n-j}(z) - n \sum_{j=n+1}^{\infty} u_j(z) u_{j-n}(z)\right] - \alpha_o (fn)^{\gamma} u_n(z) - u_n(z)/R(z) \qquad (9)$$

where u_n is the amplitude of the n^{th} harmonic of the particle velocity, z is the direction of propagation, $\beta = 1+B/2A$, c_o is the small amplitude sound velocity, R is the radius of curvature of the wavefront, α_o is the small signal absorption coefficient at 1 MHz, f is the fundamental frequency in MHz and γ is a constant usually taken to be close to 1.2 for soft tissue. For a converging wavefront R(z) is negative.

The absorbed axial power density is given by:

$$Q = -Z_T \cdot \sum_n u_n \cdot \frac{du_n}{dz} + \frac{u_n^2}{b}\frac{db}{dz} \qquad (10)$$

where Z_T is the acoustic impedance of the medium. Q is obtained by solving the rate equations (9) using (3) for u_n and du_n/dz and then evaluating (10).

In the original paper [1] it was assumed that all harmonics had the same radius of curvature as the fundamental as given by (3). Additionally the phase propagation term (8) was neglected.

A more realistic approach would seem to be to assume that each harmonic wave, except for its amplitude changes caused by nonlinear interaction, travels as a Gaussian wave independently of the other harmonics. The radius of each harmonic should thus be treated separately in (9) where from (3) and (5) it is seen that R depends on the wavelength in a direct manner. This improvement has been incorporated into the algorithms. The phase term (8) which is also frequency dependent, has also been included. The Runge-Kutta solution of (9) involves the iterative computation of u_n at $z+\Delta z$ knowing the u_n at z. This affords an opportunity to incorporate the phase propagation as determined from (8) between iterations.

RESULTS

Figure 2 describes the system. The transducer emits a Gaussian beam of diameter 0.107 metres and curvature 0.16 metres at a frequency of 0.5 MHz into water toward a tissue interface 0.06 metres away.

Figure 2

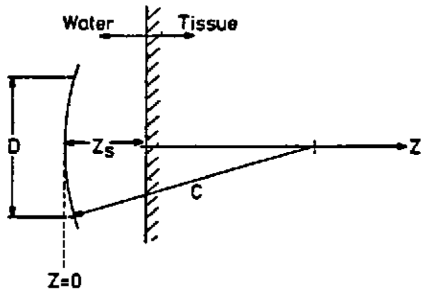

Figure 3 shows the calculated absorbed power densities on the beam axis for five axial intensities of 10^4, $10^{4.5}$, 10^5, $10^{5.5}$ and 10^6 watt/metre^2. There is weak absorption in the water followed by stronger absorption in the tissue. The APD increases with distance as far as the focus and then falls off. There is a marked enhancement in the APD near the focus for the highest and second highest intensity levels. The enhancement ratio is approximately twelve. This is significantly greater than the enhancement ratios predicted by the earlier model. Figure 4 shows the effect of increasing the frequency to 2.5 MHz. At the highest power level there is a full shock wave in the coupling water with correspondingly high APD. There is little enhancement in the region of the focal zone although the increase in APD due to focussing is clearly depicted.

It is interesting to study the shape of the particle velocity waveform.

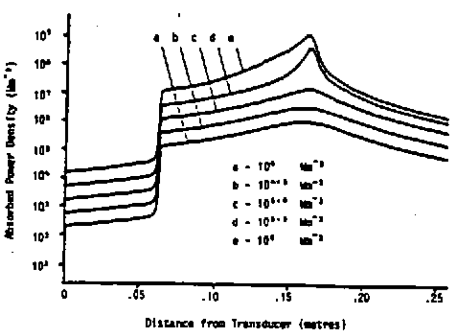

Figure 3

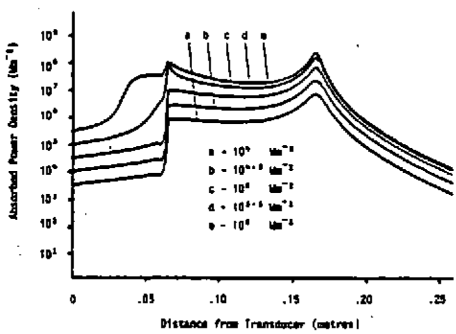

Figure 4

Figure 5 shows the wave in the neighbourhood of the focus for an axial intensity of 10^5 watts/m^2 at the transducer, a frequency of 0.5 MHz and a Gaussian beam density of 0.107 metres. The curve labelled NX=65 is at the geometric centre of curvature of the transducer. Changes in NX of unity correspond to axial displacements of 0.0025 metres with NX=1 at the transducer. The considerable asymmetry predicted with this model agrees qualitatively with the well known observed phenomenon. There is seen to be an impulsive wave profile at the focus.

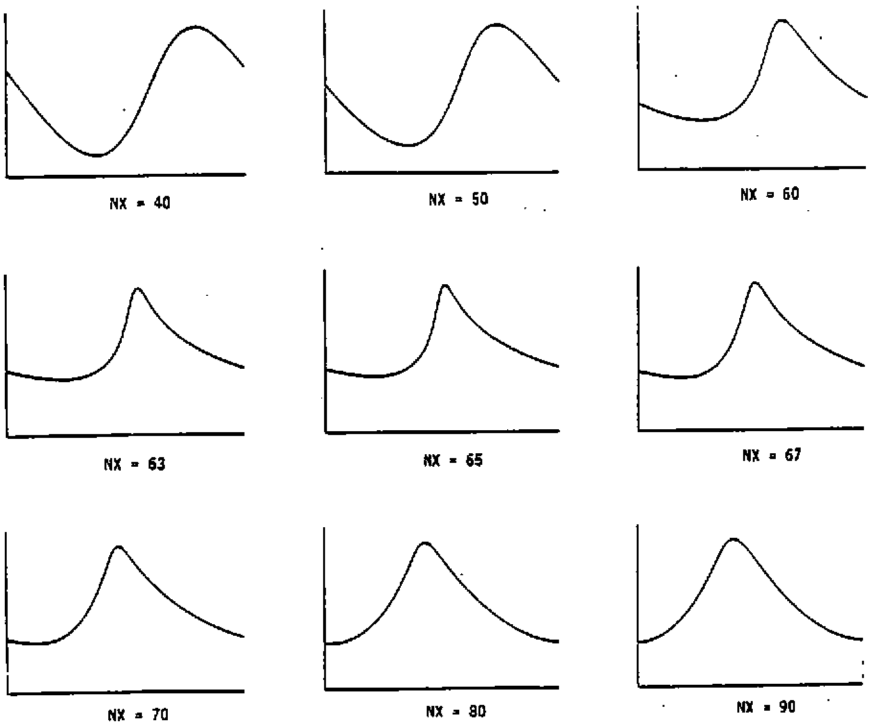

Figure 5

CONCLUSIONS

This revised model appears to be satisfactory inasmuch that it more accurately predicts the behaviour of the acoustic velocity profile. An interesting feature is that it also predicts higher enhancement ratios in the region of the beam focus than did the previous model. As such it seems likely that nonlinear effects will be useful in selectively inducing hyperthermia (also mechanical trauma) over small volumes located at depth within tissue.

REFERENCES

[1] W SWINDELL, 'A theoretical study of nonlinear effects with focused ultrasound in tissues: an "Acoustic bragg peak"', Ultrasound in Med. & Biol., Vol. 11, no. 1, 121-130, (1985).